

# HADRONIC SIGNATURES OF DECONFINEMENT STRANGENESS $s$ AND ENTROPY $S$

Quark Confinement and the Hadron Spectrum, Cagliari, Italy, September 21, 2004

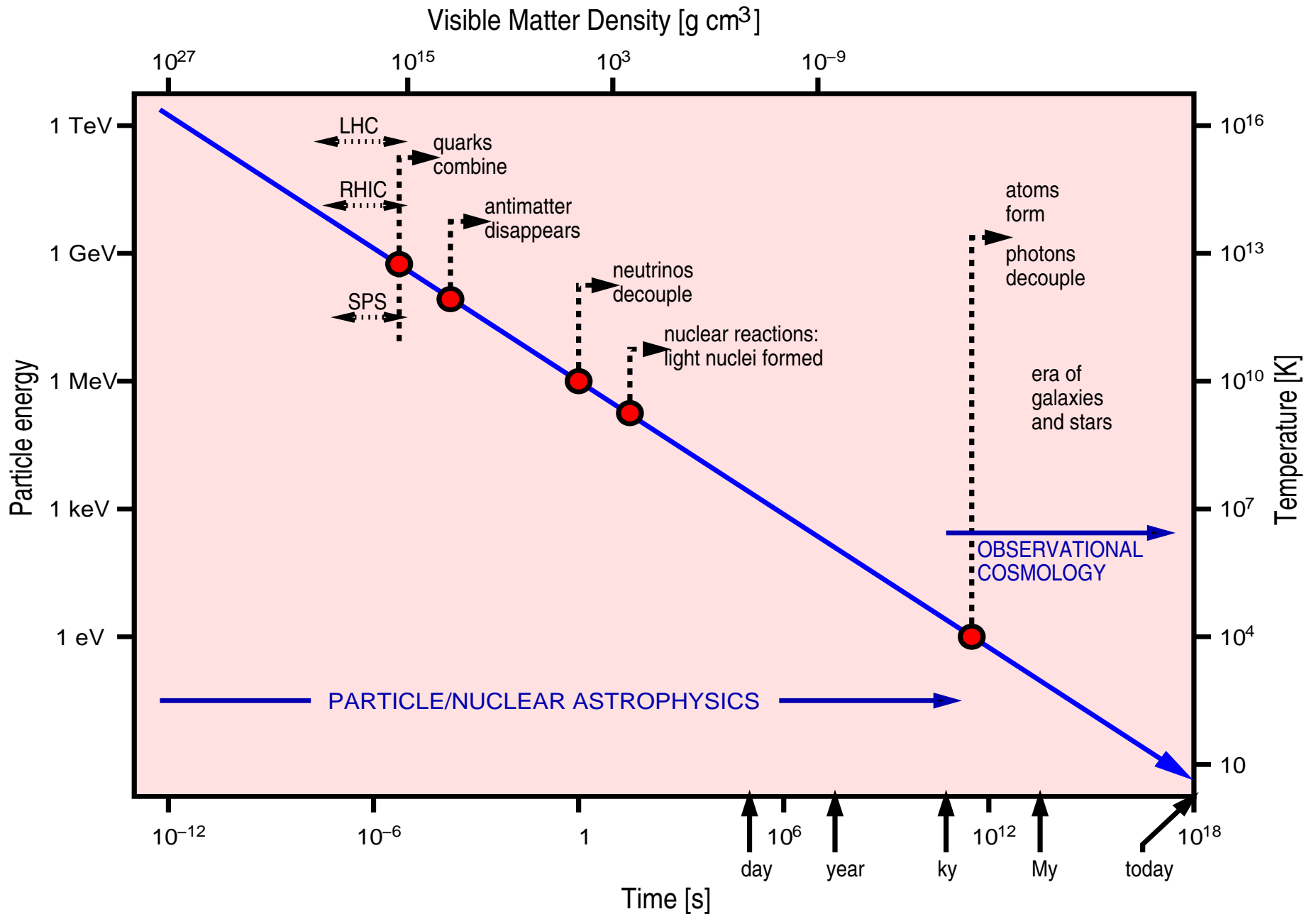
- [ I] **How and why: search for deconfinement in RHI Collisions**
- [ II] **Strangeness, entropy and resonances probes of deconfinement** p5
- [III] **Sudden hadronization and quark dynamics** p10
- [IV] **Statistical hadronization: methods, results, insights** p18
- [V] **Strangeness, entropy and QGP** p26

---

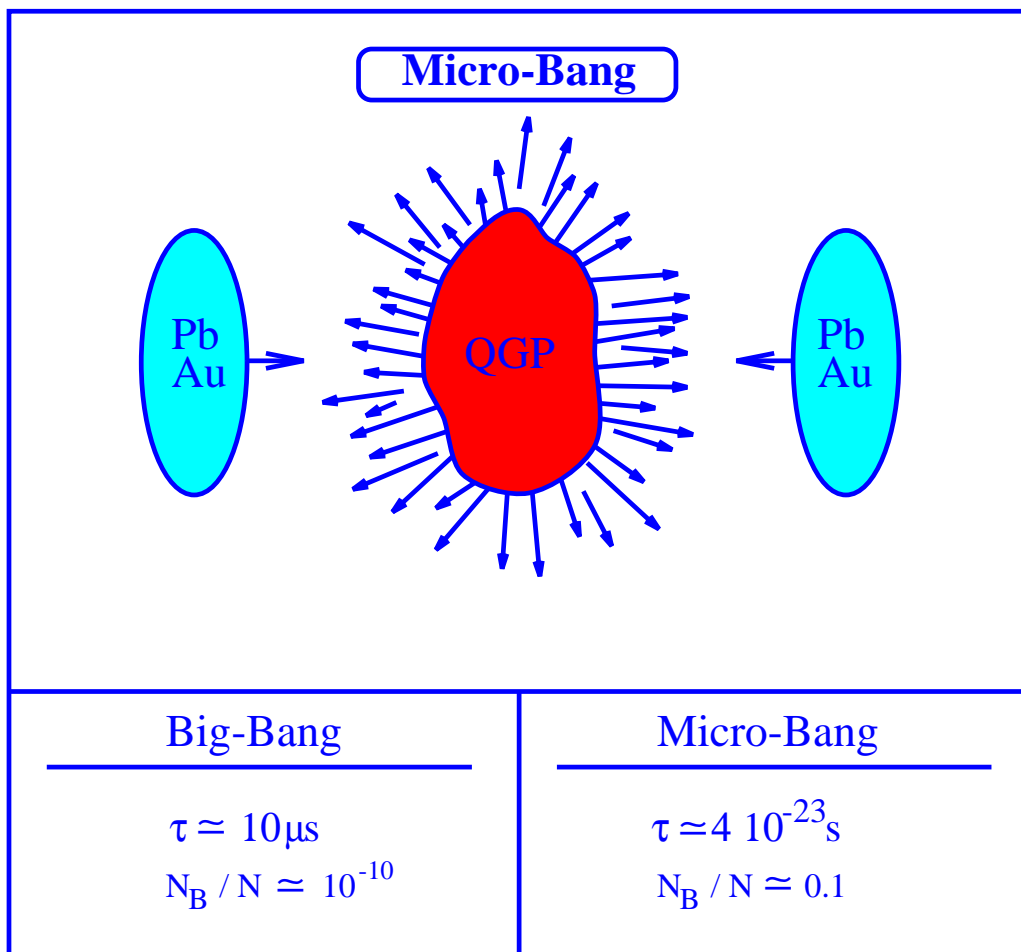
*Supported by a grant from the U.S. Department of Energy, DE-FG02-04ER41318  
In collaboration with **Jean Letessier, Paris** and **Giorgio Torrieri, Toronto***

*Johann Rafelski  
Department of Physics  
University of Arizona  
TUCSON, AZ, USA*

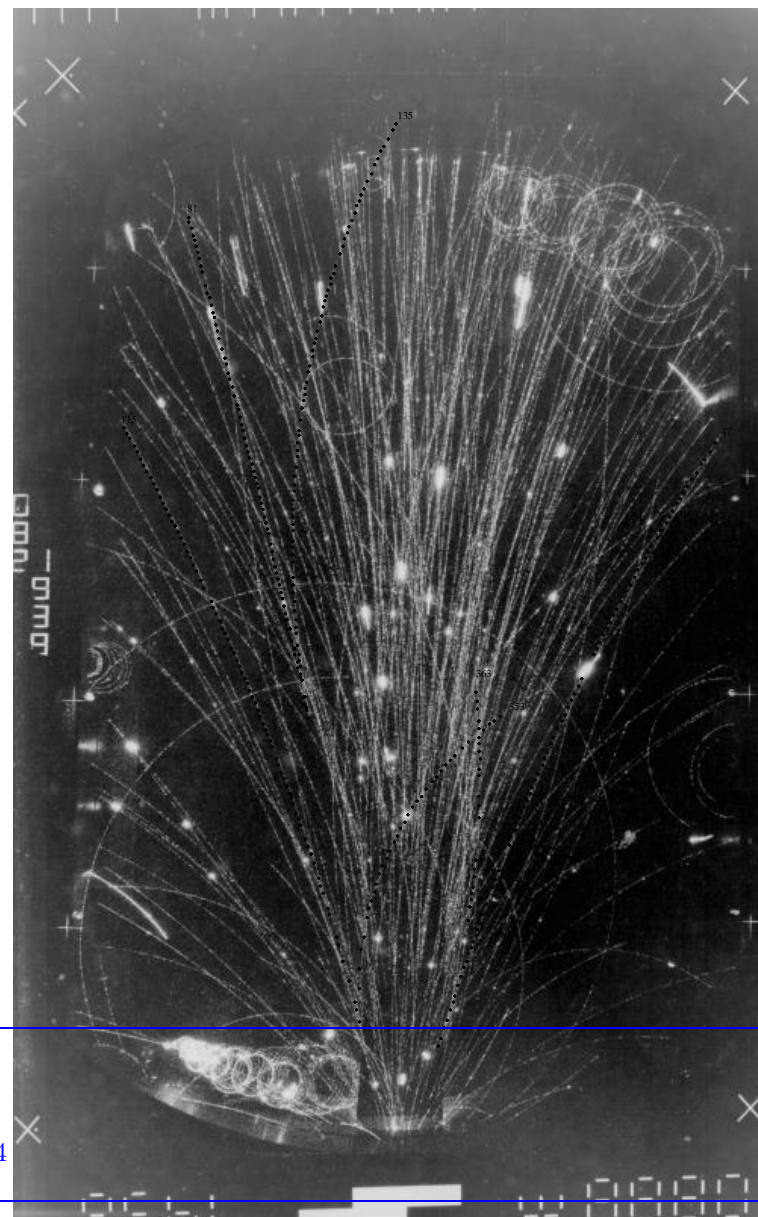
## Particle/nuclear era in the evolution of the Universe



## THE EARLY DECONFINED UNIVERSE IN THE LABORATORY



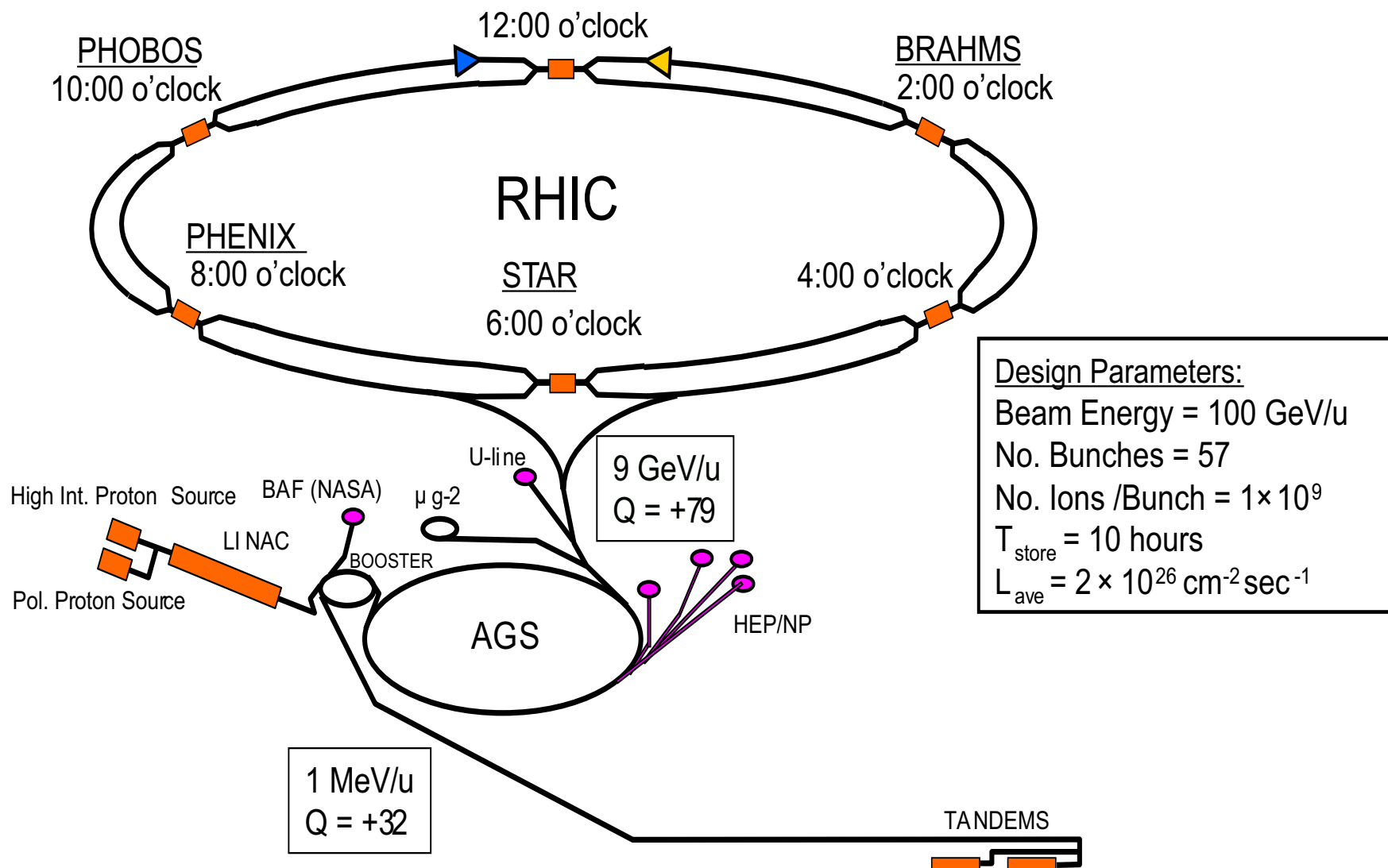
Order of Magnitude



Reinhard Stock NA35 1986: S-Ag at 200 AGeV

|                       |            |  |
|-----------------------|------------|--|
| <b>ENERGY density</b> | $\epsilon$ | $\approx 1-5 \text{ GeV}/\text{fm}^3 = 1.8-9 \cdot 10^{15} \text{ g}/\text{cc}$  |
| Latent vacuum heat    | $B$        | $\approx 0.1-0.4 \text{ GeV}/\text{fm}^3 \approx (166-234 \text{ MeV})^4$  |
| <b>PRESSURE</b>       | $P$        | $= \frac{1}{3}\epsilon = 0.52 \cdot 10^{30} \text{ barn}$  |
| <b>TEMPERATURE</b>    | $T_0, T_f$ | 300-250, 175-145 MeV; <span style="color: green;">300 MeV <math>\approx</math> 3.5 <math>\cdot 10^{12}</math> K</span> |

# BROOKHAVEN NATIONAL LABORATORY



**RHIC: Relativistic Heavy Ion Collider  $20 < \sqrt{s_{NN}} < 200$  A-A**

## Deconfinement

We aim to verify experimentally the theory paradigm:  
the QCD Vacuum structure is the origin of **quark confinement**.

**What/where is deconfinement?**

A domain of (space, time) much larger than normal hadron size in which color-charged quarks and gluons are propagating, constrained by external 'frozen vacuum' which abhors color.

We expect a pronounced boundary in temperature and density between confined and deconfined phases of matter: **phase diagram**. Deconfinement expected at both high temperature and at high matter density.

In a finite size system expect in general a 'transformation', not a sharp boundary.

What we need as background knowledge:

- 1) Hot QCD in equilibrium (quark-gluon plasm, QGP) from QCD-lattice,
- 2) Understanding how to adapt QGP to the non-equilibrium heavy ion reactions,
- 3) Understanding of hadronization dynamics and final particle yields,
- 4) Identify sensitive (hadronic and other) signatures of deconfinement

beware: final particles always hadrons

**NOT A SINGLE SMOKING GUN type observation, NOT a 'new particle'.**

## Hadronic observables: STRANGENESS $s$ AND ENTROPY $S$

Stable matter is made of only up and down quarks, strange flavor is always almost all newly made. In the QGP hadrons are dissolved

into an entropy rich partonic liquid. Once entropy has been created in the breaking of color bonds, it cannot decrease, appears in hadron multiplicity.

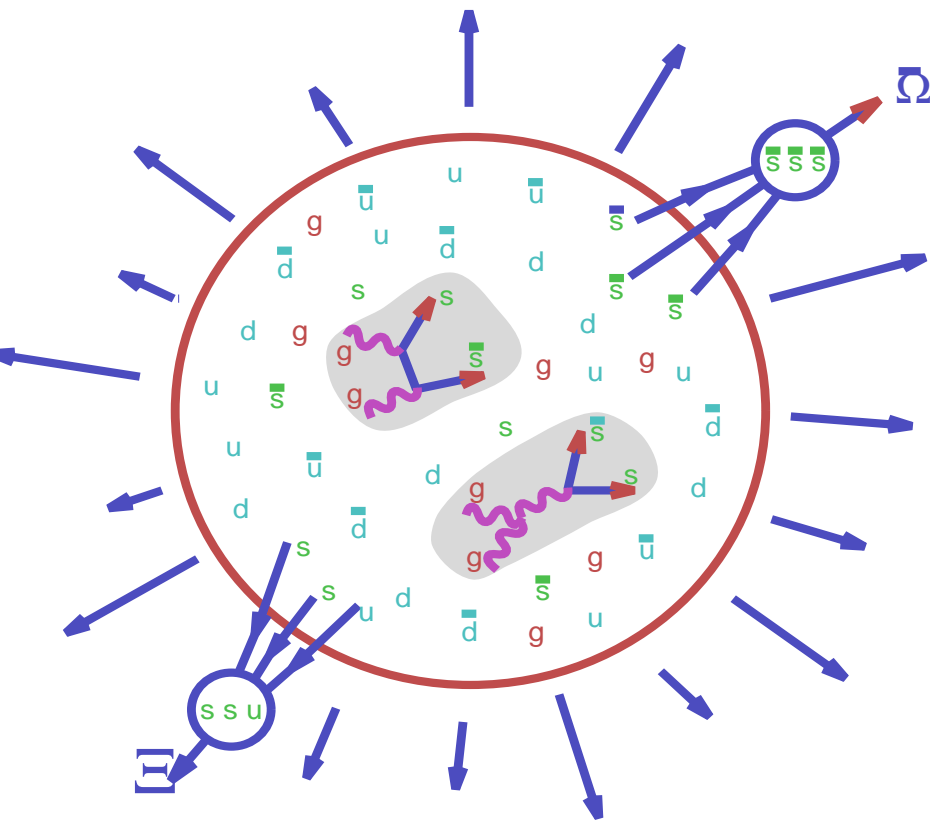
TWO STEP MECHANISM of (strange) hadron formation from QGP:

1.  $GG \rightarrow s\bar{s}$  in QG-plasma
2. hadronization of pre-formed  $s, \bar{s}$  quarks

**RESULT:** Excess of strangeness and even more of complex rarely produced multi strange (anti)particles from QGP **enabled by coalescence of**

$s, \bar{s}$  quarks made earlier in QCD based microscopic reactions.

**IN REVERSE:** strangeness enhancement indicates presence of gluons (specific for deconfinement) as a new strangeness producing source, and strange antibaryon enhancement indicated coalescence which is a signature of quark mobility in the source volume.

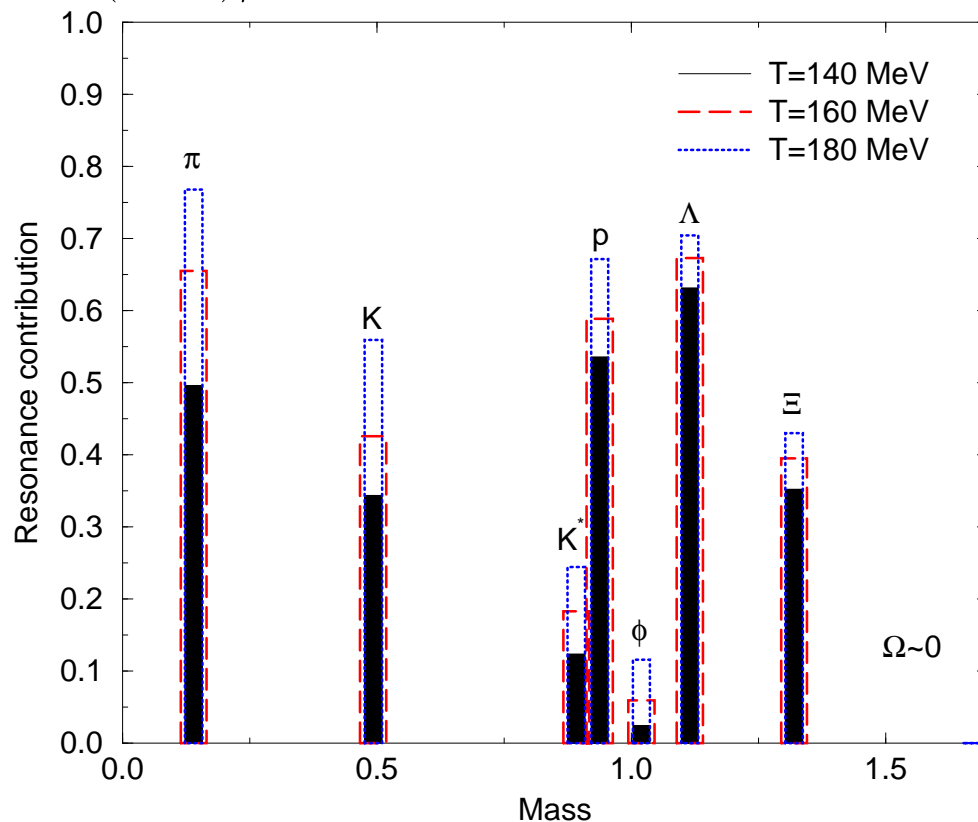


## Hadronic observables: Resonances

Statistical Hadronization Hypothesis: particle production (both (relative) yields and spectra) can be described by maximizing the accessible phase space, **This is the Fermi-Hagedorn model.**

### **TEST AND USE OF STATISTICAL HADRONIZATION MODEL**

Particle yields with same valance quark content are in relative chemical equilibrium, e.g. the relative yield of  $\Delta(1230)/N$  as of  $K^*/K$ ,  $\Sigma^*(1385)/\Lambda$ , etc, is controlled by chemical freeze-out temperature  $T$ :



$$\frac{N^*}{N} = \frac{g^*(m^*T)^{3/2}e^{-m^*/T}}{g(mT)^{3/2}e^{-m/T}}$$

Resonances decay rapidly into 'stable' hadrons and dominate the yield of most stable hadronic particles.

Resonances test first statistical hadronization principle and beyond, **characterize the dynamics of QGP hadronization.**

## OBSERVABLE RESONANCE YIELDS

Invariant mass method: construct invariant mass from decay products:

$$M^2 = (\sqrt{m_a^2 + \vec{p}_a^2} + \sqrt{m_b^2 + \vec{p}_b^2} + \dots)^2 - (\vec{p}_a + \vec{p}_b + \dots)^2$$

If one of decay products rescatter the reconstruction not assured.  
**Apparent ‘suppression’ of resonance production.**

Strongly interacting matter essentially non-transparent. Simplest model: If resonance decays within matter, resonance disappears from view. **Implementation Attenuation of yield  $N^*$  seen in channel involving final Decay state  $N^* \rightarrow D + \dots$ ;  $\Gamma$  is  $N^*$  in matter width,  $N^*(t=0)$  given by statistical hadronization,  $D(t=0) = 0$ :**

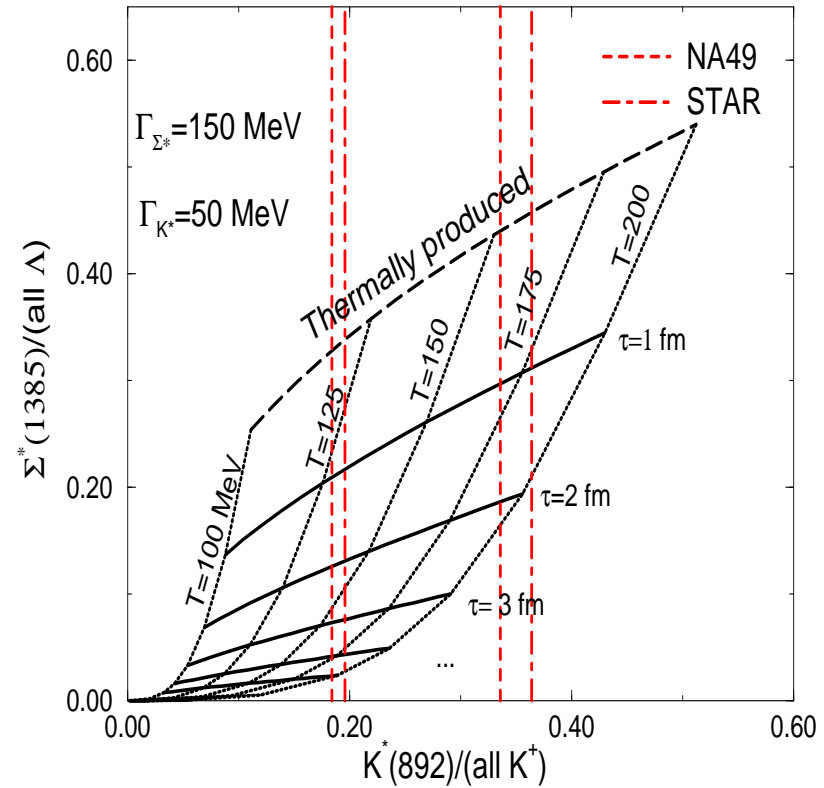
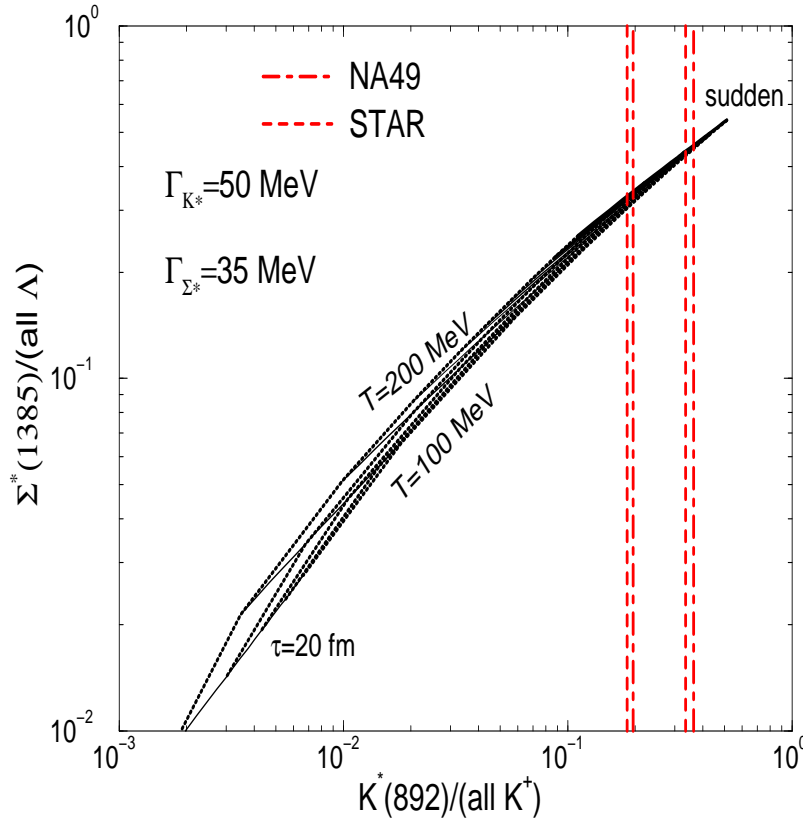
$$\frac{dN^*}{dt} = -\Gamma N^* + R, \quad \frac{dD}{dt} = \Gamma N^* - D \sum_j \langle \sigma_{Dj} v_{Dj} \rangle \rho_j \left( \frac{R_0}{R_0 + v_c t} \right)^3$$

**In the loss term, the last factor dilutes the density of scattering matter by collective expansion with velocity  $v_c$ , here shown in 3D. Integrate to time  $t = \tau$ , the time spend in the opaque matter. This time can be interpreted as the time it takes the particle  $N^*$  to escape into free space. **Regeneration term  $R \propto \langle \sigma_{Di}^{INEL} v_{Di} \rangle \rho_i$  much smaller since real production required,  $\{i\} \ll \{j\}$ .****

**TWO resonance ratios combined**

natural widths

spread  $\Gamma_{\Sigma^*} = 150$  MeV



Dependence of the combined  $\Sigma^*/(\text{all } \Lambda)$  with  $K^*(892)/(\text{all } K)$  signals on the chemical freeze-out temperature and HG phase lifetime.

Even the first rough measurement of  $K^*/K$  indicates that there is no long lived hadron phase. In matter widening makes this conclusion stronger.

**We are lead to: Sudden Hadronization of QGP**

Other evidence for sudden hadronization - hadron emission directly into free space:

CERN SPS Experiments since 1991 (WA85, WA97, NA57, NA49) see identical shape of  $m_{\perp}$  spectra of strange baryons and antibaryons, obtained in central reactions at CM rapidity, also observed at RHIC.

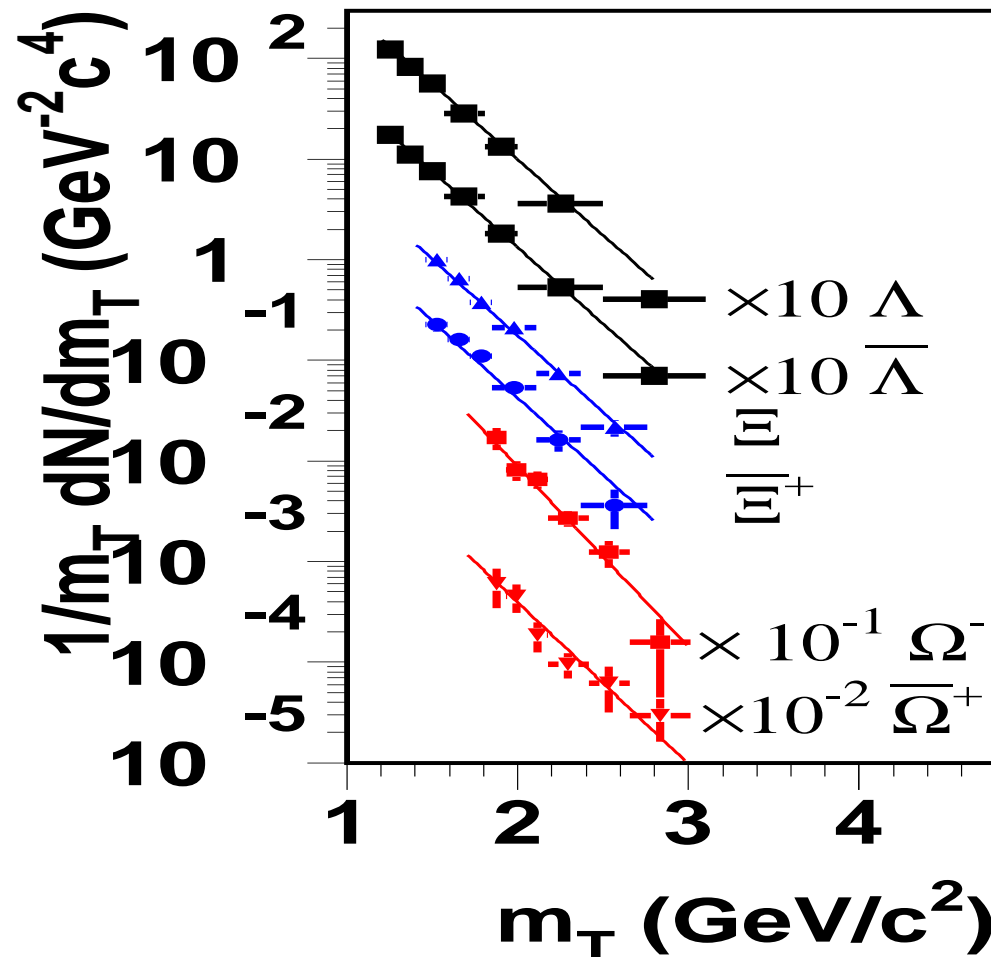
Interpretation: Common matter-antimatter formation mechanism, little reannihilation in sequel evolution.

Antibaryon appears to be DIRECTLY EMITTED by a quark source into vacuum.

Fast hadronization confirmed further by HBT particle correlation analysis, which yields a nearly energy independent size of hadron fireball with short lifespan of pion production.

# High $m_{\perp}$ matter-antimatter slope universality: SPS

| WA97                      | $T_{\perp}^{\text{Pb}}$ [MeV] |
|---------------------------|-------------------------------|
| $T^{\Lambda}$             | $289 \pm 3$                   |
| $T^{\bar{\Lambda}}$       | $287 \pm 4$                   |
| $T^{\Xi}$                 | $286 \pm 9$                   |
| $T^{\bar{\Xi}}$           | $284 \pm 17$                  |
| $T^{\Omega+\bar{\Omega}}$ | $251 \pm 19$                  |



$\Lambda$  within 1% of  $\bar{\Lambda}$

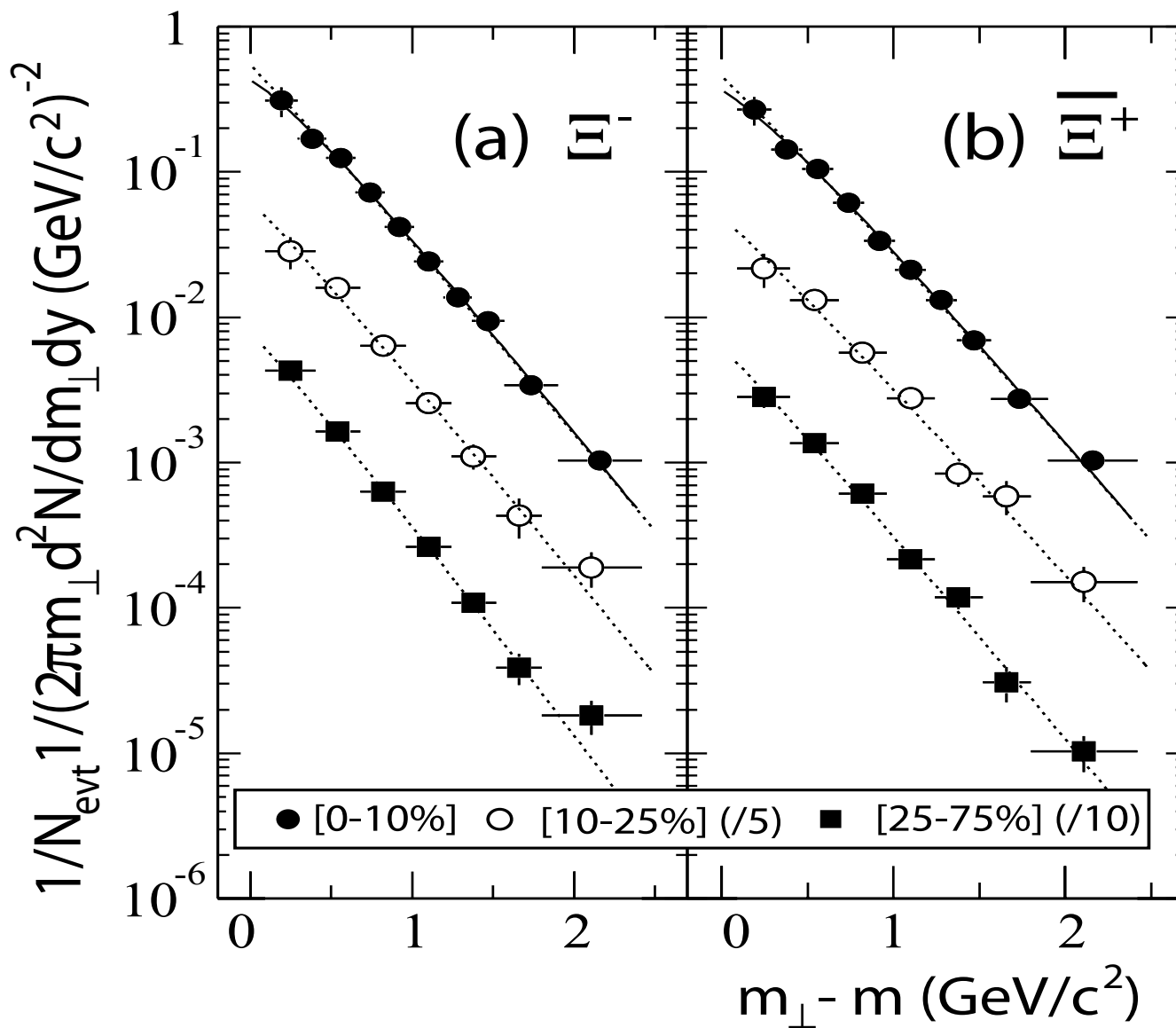
**Spectra at RHIC-STAR 130+130 A GeV show the same effect**

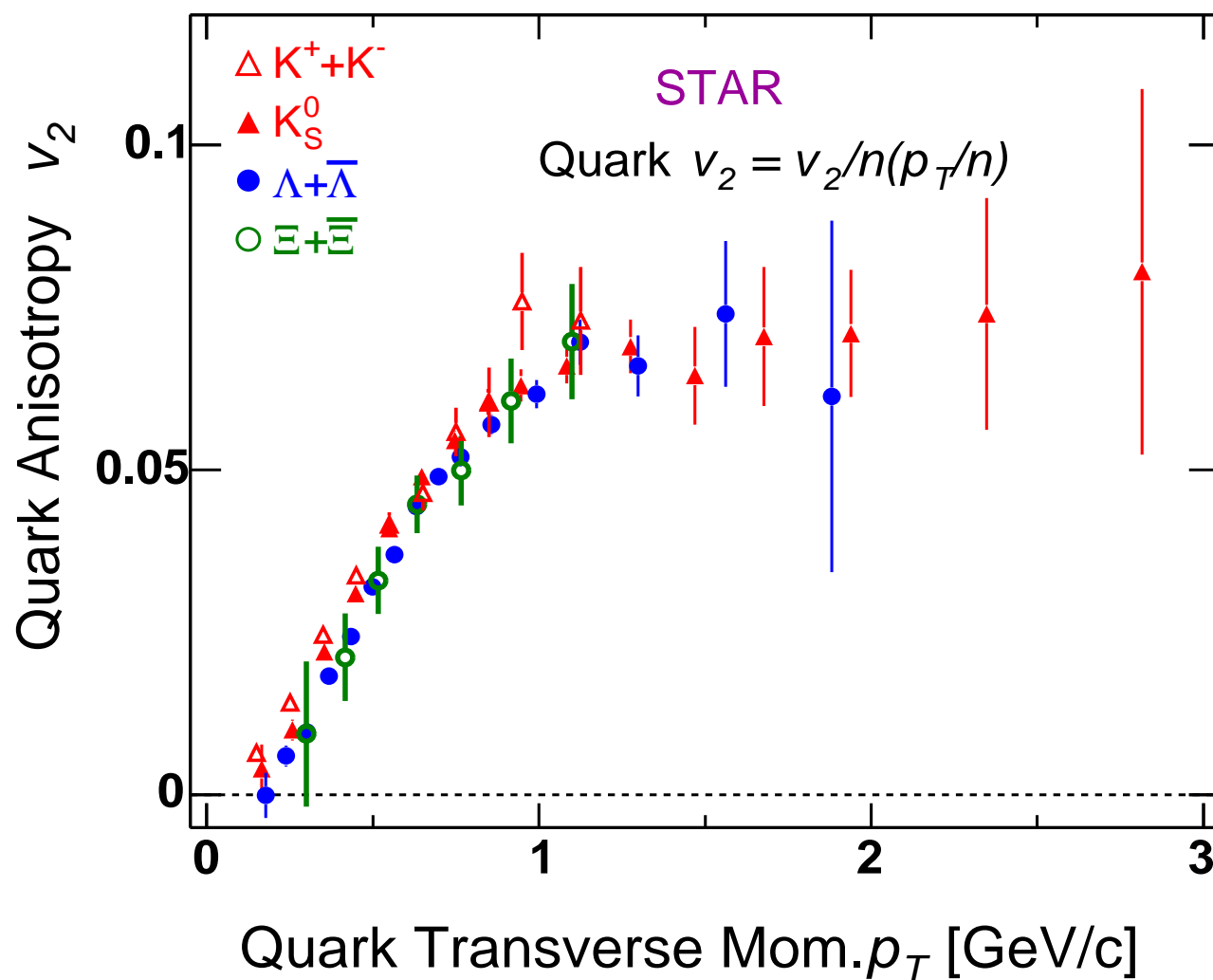
| $h^-$           | Exponential Fit |                 | Boltzmann Fit     |                 |                   |
|-----------------|-----------------|-----------------|-------------------|-----------------|-------------------|
|                 | centrality      | $dN/dy$         | $T_E(\text{MeV})$ | $dN/dy$         | $T_B(\text{MeV})$ |
| $260.3 \pm 7.5$ | $\Xi^-$         | $2.16 \pm 0.09$ | $338 \pm 6$       | $2.06 \pm 0.09$ | $296 \pm 5$       |
|                 | $\bar{\Xi}^+$   | $1.81 \pm 0.08$ | $339 \pm 7$       | $1.73 \pm 0.08$ | $297 \pm 5$       |
| $163.6 \pm 5.2$ | $\Xi^-$         | $1.22 \pm 0.11$ | $335 \pm 16$      | $1.18 \pm 0.11$ | $291 \pm 13$      |
|                 | $\bar{\Xi}^+$   | $1.00 \pm 0.10$ | $349 \pm 17$      | $0.97 \pm 0.10$ | $302 \pm 13$      |
| $42.5 \pm 3.0$  | $\Xi^-$         | $0.28 \pm 0.02$ | $312 \pm 12$      | $0.27 \pm 0.02$ | $273 \pm 10$      |
|                 | $\bar{\Xi}^+$   | $0.23 \pm 0.02$ | $320 \pm 11$      | $0.22 \pm 0.02$ | $280 \pm 9$       |

$m_\perp$  spectra of  $\Xi^-$ ,  $\bar{\Xi}^-$ , for three centrality bins 0-10%, 10-25% and 25-75% with  $h^- = dN_{h^-}/d\eta|_{|\eta|<0.5}$ . Statistical and  $p_\perp$  dependent systematic uncertainties are presented. The  $p_\perp$  independent systematic uncertainties are 10%.

(STAR Collaboration, PRL92 (2004) 182301)

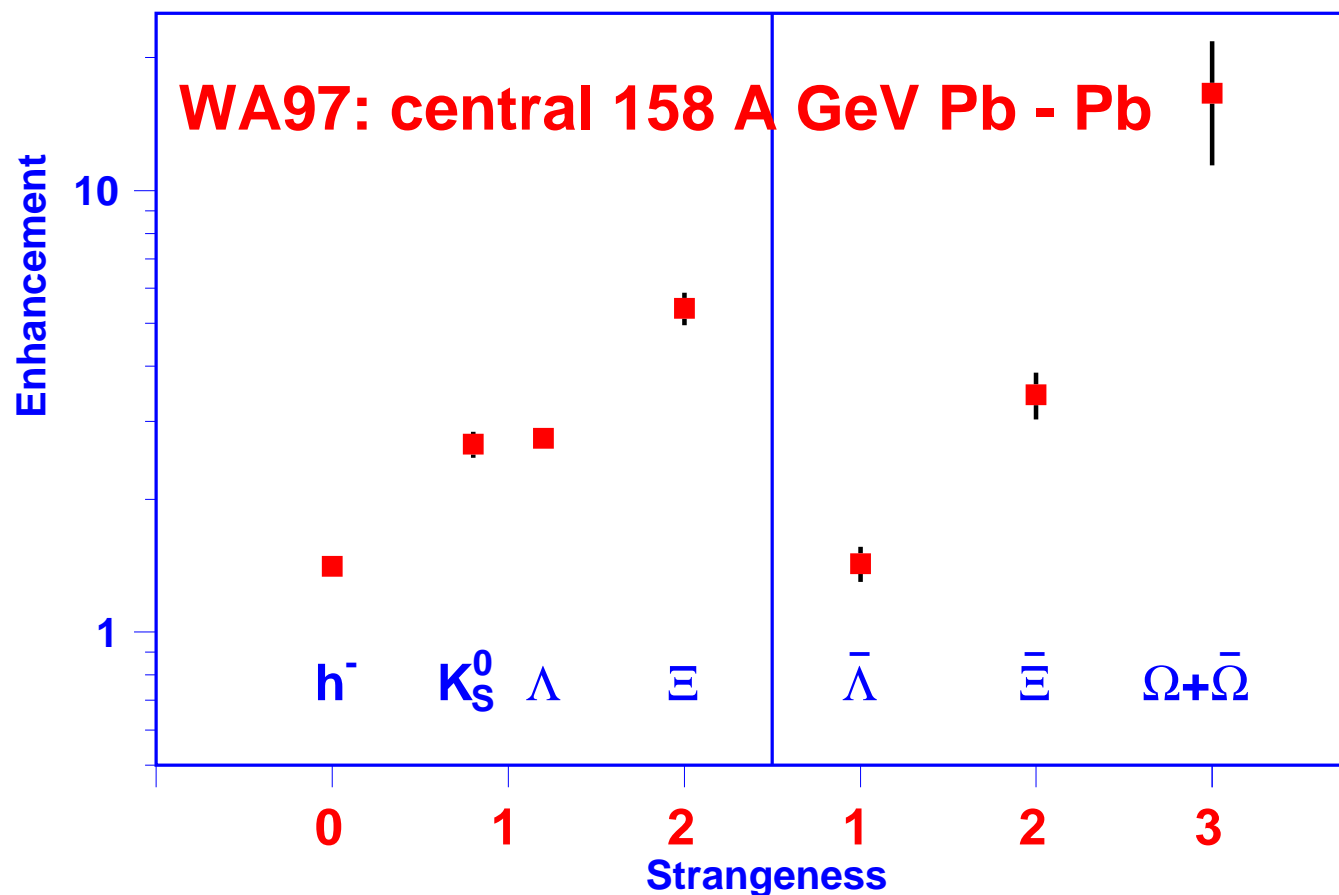
$\Xi^-, \bar{\Xi}^-$  Spectra RHIC-STAR 130+130 A GeV



**Azimuthal asymmetry of particle spectra**

The asymmetry appears as due to quark content, is common in magnitude for  $q, \bar{q}, s, \bar{s}$ . Evidence for bulk matter flow at partonic level. See talk by Huan-Zhong Huang Friday, session D

## (MULTI)STRANGE (ANTI)HYPERON ENHANCEMENT



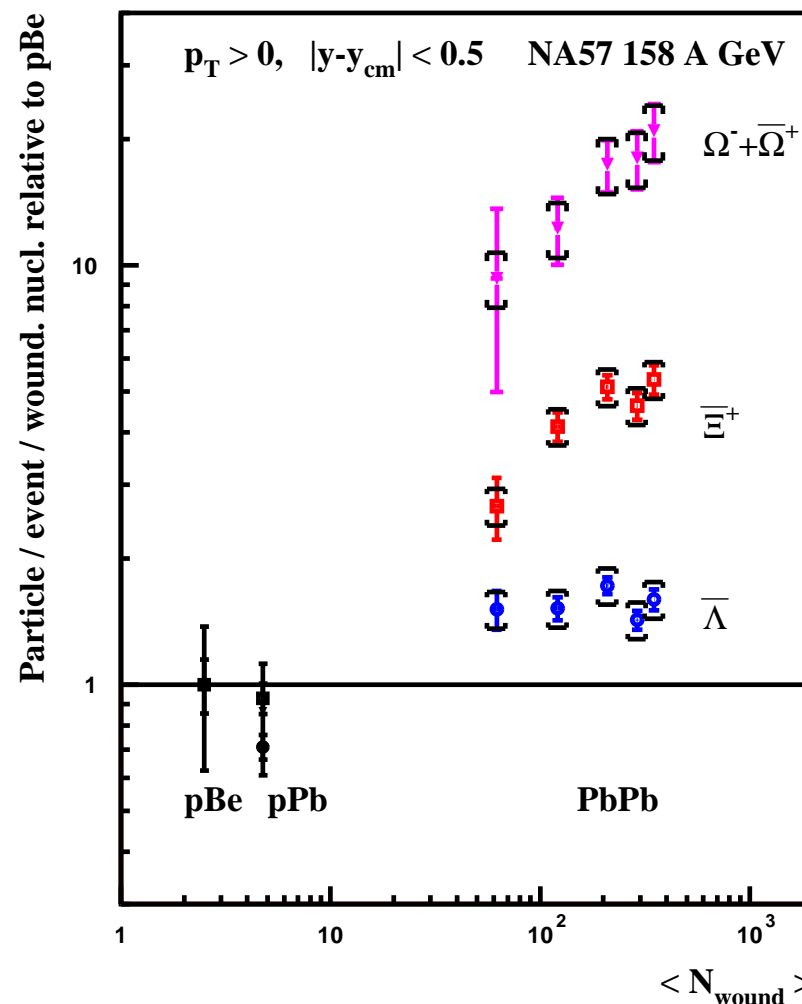
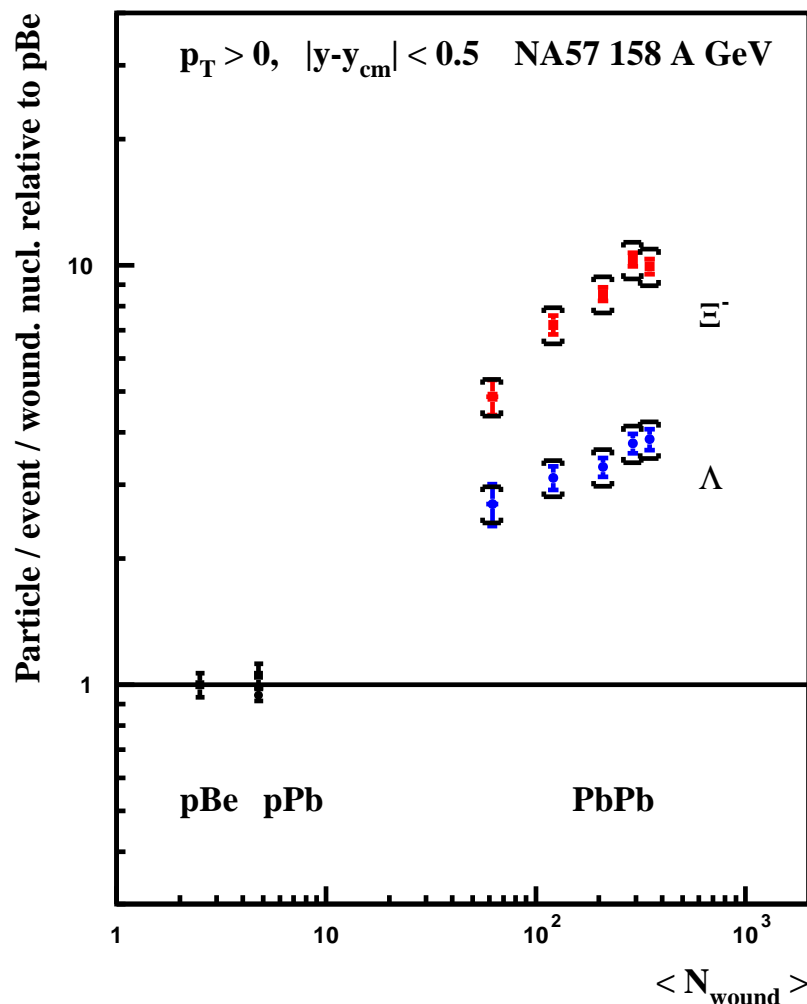
Enhancement GROWTH with

strangeness

antiquark content.

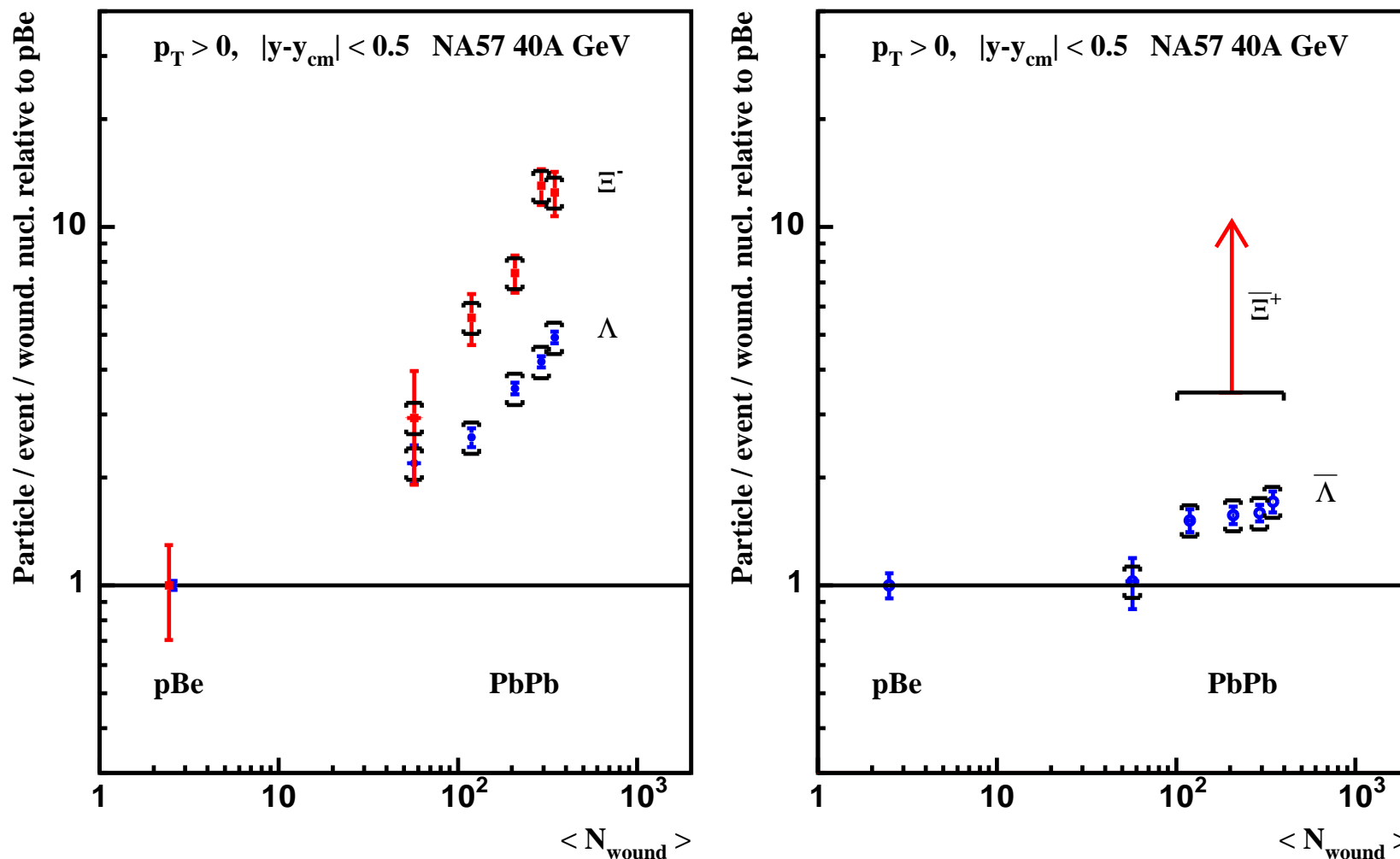
Enhancement is here defined with respect to the yield in p-Be collisions, scaled up with the number of collision 'wounded' nucleons.

## ENHANCEMENT AS FUNCTION OF REACTION VOLUME



Note the gradual onset of enhancement with reaction volume. “Canonical enhancement” (a hadronic equilibrium model) is grossly inconsistent with these results. Gradual enhancement shown predicted by kinetic strangeness production.

## ENHANCEMENT at low SPS Energy



At 40A GeV we still see a strong volume dependent hyperon enhancement, in agreement with expectations for deconfined state formation.

## DIRECT PARTICLE PRODUCTION

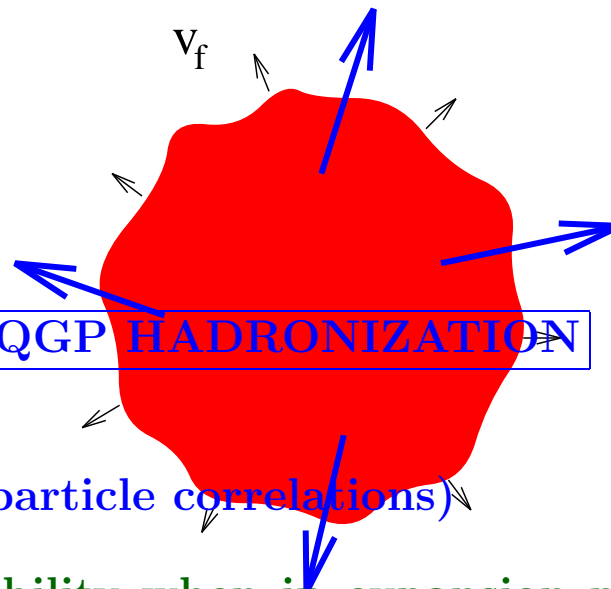
Common formation mechanism for all particles, flow at quark level, for antimatter little reannihilation in sequel evolution.

Appears to be direct emission by a quark source into vacuum.

Practically no hadronic 'phase'!

No 'mixed phase' either!

Direct emission of free-streaming hadrons from **exploding QGP**



Develop analysis tools viable in SUDDEN QGP HADRONIZATION

SLOW transformation is in contradiction to experiment (single particle spectra, 2-particle correlations)

Reaction mechanism: filamentation instability when in expansion pressure reverses (L. Csernai, Bergen et al, JR et al).

NEXT:

Quark chemistry and **Statistical Hadronization**

## Quark chemistry: chemical potentials $\equiv$ fugacities

particle fugacity:  $\Upsilon_i \equiv e^{\sigma_i/T} \iff \sigma_i$  particle 'i' chemical potential

Example of NUCLEONS:

two particles  $N, \bar{N} \rightarrow$  two chemical factors, a convenient choice is:

$$\sigma_N \equiv \mu_b + T \ln \gamma_N, \quad \sigma_{\bar{N}} \equiv -\mu_b + T \ln \gamma_N;$$

$$\Upsilon_N = \gamma_N e^{\mu_b/T}, \quad \Upsilon_{\bar{N}} = \gamma_N e^{-\mu_b/T}.$$

The (baryo)chemical potential  $\mu_b$  controls the particle difference = **baryon number**. This can be seen looking at the first law of thermodynamics:

$$\begin{aligned} dE + P dV - T dS &= \sigma_N dN + \sigma_{\bar{N}} d\bar{N} \\ &= \mu_b (dN - d\bar{N}) + T \ln \gamma_N (dN + d\bar{N}). \end{aligned}$$

$\gamma$  regulates the number of nucleon-antinucleon pairs present.

Quark fugacities  $\iff$  Hadron fugacities

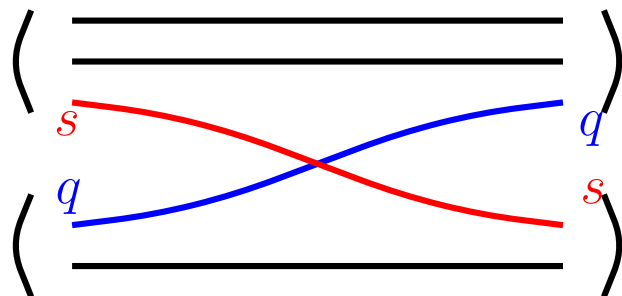
$$e^{\mu_b/T} = \lambda_q^3, \quad \lambda_q^2 = \lambda_u \lambda_d, \quad \mu_S = \frac{\mu_b}{3} - \mu_s$$

Counting particles easier counting quark content ( $u, d, s, \dots$ )

# FOUR QUARKS: $s, \bar{s}, q, \bar{q} \rightarrow$ FOUR CHEMICAL PARAMETERS

|  |                                  |
|--|----------------------------------|
| $\gamma_i$ controls overall abundance<br>of quark ( $i = q, s$ ) pairs                   | Absolute chemical<br>equilibrium |
| $\lambda_i$ controls difference between<br>strange and non-strange quarks ( $i = q, s$ ) | Relative chemical<br>equilibrium |

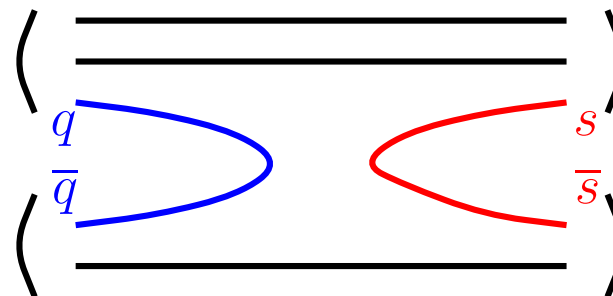
**HG-EXAMPLE: redistribution,**  
**Relative** chemical equilibrium



**EXCHANGE REACTION**

$\lambda_i$

**production of strangeness**  
**Absolute** chemical equilibrium



**PAIR PRODUCTION REACTION**

$\gamma_i$

## PARTICLE ABUNDANCES

$$\pi(q\bar{q}) \sim \gamma_q^2 \quad N(qqq) \sim \gamma_q^3 \lambda_q^3; \quad \bar{N}(\bar{q}\bar{q}\bar{q}) \sim \gamma_q^3 \lambda_q^{-3}$$

## QUANTUM STATISTICS

$$\frac{N_\pi}{V} = g_\pi \int \frac{d^3p}{(2\pi)^3} \frac{1}{\gamma_q^{-2} e^{\sqrt{m_\pi^2 + p^2}/T} - 1}, \quad \gamma_q^2 < e^{m_\pi/T} \simeq (1.6)^2$$

$$\frac{N}{V} = g_N \int \frac{d^3p}{(2\pi)^3} \frac{1}{1 + \gamma_q^{-3} \lambda_q^{-3} e^{E/T}} \quad \frac{\bar{N}}{V} = g_N \int \frac{d^3p}{(2\pi)^3} \frac{1}{1 + \gamma_q^{-3} \lambda_q^{+3} e^{E/T}}$$

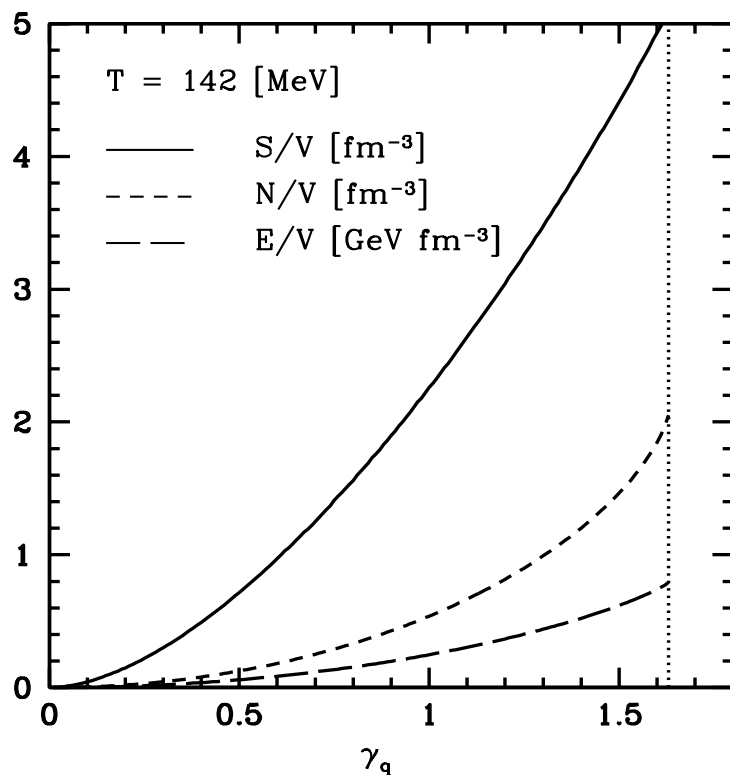
$$\mu_N^{\text{eff}} = 3T(\ln \lambda_q + \ln \gamma_q); \quad \mu_{\bar{N}}^{\text{eff}} = -3T(\ln \lambda_q - \ln \gamma_q)$$

presence of  $\gamma, \lambda$  is simply allowing to assign different potentials for particles and antiparticles else  $\bar{\mu} = -\mu$

Need to find a way to ‘consume’ excess of QGP entropy

Maximization of entropy density in emitted pions.  $E_\pi = \sqrt{m_\pi^2 + p^2}$

$$S_{B,F} = \int \frac{d^3p d^3x}{(2\pi\hbar)^3} [\pm(1 \pm f) \ln(1 \pm f) - f \ln f], \quad f_\pi(E) = \frac{1}{\gamma_q^{-2} e^{E_\pi/T} - 1}.$$



Pion phase space properties  
as function of  $\gamma_q$ .

SPECIAL ROLE OF  $\gamma_q^2 \rightarrow e^{m_\pi/T}$

When QGP turns into hadrons somehow the extra COLOR degrees of freedom need to manifest their presence! There is to be a way to ‘consume’ QGP entropy (e.g., excess of degrees of freedom) in absence of slow hadronization (no volume expansion).

## Particle ratios sensitive to chemical parameters

$$R_\Lambda = \frac{\bar{\Lambda}}{\Lambda} = \frac{\bar{\Lambda} + \bar{\Sigma}^0 + \bar{\Sigma}^* + \dots}{\Lambda + \Sigma^0 + \Sigma^* + \dots} = \frac{\bar{s}\bar{q}\bar{q}}{sqq} = \lambda_s^{-2} \lambda_q^{-4} = e^{2\mu_s/T} e^{-2\mu_b/T} .$$

$$R_\Xi = \frac{\bar{\Xi}^-}{\Xi^-} = \frac{\bar{\Xi}^- + \bar{\Xi}^* + \dots}{\Xi^- + \Xi^* + \dots} = \frac{\bar{s}\bar{s}\bar{q}}{ssq} = \lambda_s^{-4} \lambda_q^{-2} = e^{4\mu_s/T} e^{-2\mu_b/T} .$$

Occupancy fugacities  $\gamma_q, \gamma_s$  relevant when comparing particles with different flavor  $q, s$  quark content:

$$\frac{\Xi^-(dss)}{\Lambda(dds)} = \frac{\gamma_d \gamma_s^2}{\gamma_d^2 \gamma_s} \frac{\lambda_d \lambda_s^2}{\lambda_d^2 \lambda_s} \frac{\sum_i g_i^\Xi (m_i^\Xi)^2 K_2(m_i^\Xi/T)}{\sum_i g_i^\Lambda (m_i^\Lambda)^2 K_2(m_i^\Lambda/T)} .$$

However, sensitivity not only to  $\gamma_s/\gamma_q$  requires comparison of baryons with mesons

## Complete description of all hadron yields

We note above the presence of resonance decays. Full analysis requires a significant effort with 1000's of decaying states. A public package **SHARE** Statistical Hadronization with Resonances is available at <http://www.physics.arizona.edu/~torrieri/SHARE/share.html> developed by Kraków-Tucson collaboration.

Lead author: **Giorgio Torrieri.**

---

The **complete** statistical hadronization model allows precise description of all hadron yields, including resonances at all energies. The myth that resonances are not described within the same scheme is due to the limited model applied by some other groups which omits one or more key properties required. We find that Single freeze-out model as proposed in 1991 suffices when we consider:

1. Complete tree of resonance decays please note:  
not only for yields but also most important for **spectra**.
2. **WIDTH** of the resonances (needed to describe resonance yields)
3. Chemical off-equilibrium in hadron yields: expect **QGP** near equilibrium, hence in general non-equilibrium yields for the final state hadrons sector (see below).

Look for forthcoming publications using the SHARE package

## Particle ratios in a global fit of statistical parameters: SHARE

$\sqrt{s_{NN}} = 130$  GeV experimental hadron ratios, in comparison with the statistical hadronization models.  $K_{S,L}$ , and  $Y \rightarrow \pi$  contributions have been corrected in the experimental result,  $Y \rightarrow$  baryon have not.

| particle ratio                                | compl. model              |        | (theory – experiment)/(experimental error) |                  |                           |                 |                                 |                 |                 |
|---|---------------------------|--------|--|------------------|---------------------------|-----------------|---------------------------------|-----------------|-----------------|
|   | exp.                      | error  | $\gamma_q$ and $\gamma_s$ vary             |                  | $\gamma_q = \gamma_s = 1$ |                 | $\gamma_q = 1, \gamma_s$ varies |                 |                 |
|   |                           |        | $\Gamma = 0$                               | $\Gamma \neq 0$  | $\Gamma = 0$              | $\Gamma \neq 0$ | $\Gamma = 0$                    | $\Gamma \neq 0$ |                 |
| $\pi^-/\pi^+$                                 | 0.9935                    | 1.0000 | 0.02                                       | -0.3255          | -0.3252                   | -0.3685         | -0.3628                         | -0.4093         | -0.3868         |
| $\Xi/\pi^-$                                   | 0.0095                    | 0.0093 | 0.002                                      | 0.0680           | 0.1217                    | -0.5734         | -0.4255                         | -0.0554         | -0.0413         |
| $\Xi/\pi^-$                                   | 0.0072                    | 0.0080 | 0.0017                                     | -0.4172          | -0.3731                   | -0.9447         | -0.8287                         | -0.5096         | -0.5005         |
| $\Xi/\Xi$                                     | 0.7711                    | 0.8530 | 0.10                                       | -0.8035          | -0.8185                   | -0.6877         | -0.7288                         | -0.7669         | -0.7800         |
| $\frac{\Omega+\bar{\Omega}}{\Xi+\bar{\Xi}}$   | 0.1526                    | 0.1438 | 0.035                                      | 0.2021           | 0.2509                    | -0.2784         | -0.2674                         | 0.1621          | -0.0247         |
| $\frac{\Xi+\bar{\Xi}}{\Lambda+\bar{\Lambda}}$ | 0.1588                    | 0.187  | 0.046                                      | -0.6135          | -0.5922                   | -1.1202         | -1.1933                         | -0.8698         | -0.9724         |
| $\Xi/\Lambda$                                 | 0.1664                    | 0.215  | 0.054                                      | -0.9008          | -0.8820                   | -1.1975         | -1.3814                         | -1.1089         | -1.2002         |
| $\Xi/\phi$                                    | 0.3523                    | 0.34   | 0.07                                       | -0.2007          | 0.1758                    | -0.0579         | -0.1596                         | -0.4875         | -0.4647         |
| $K^+/p$                                       | 1.9829                    | 2.4    | 0.5  | -0.7901          | -0.8342                   | -1.8733         | -1.7046                         | -1.1776         | -1.1626         |
| $K^+/\bar{p}$                                 | 2.8632                    | 3.     | 0.5  | -0.2138          | -0.2736                   | -1.6992         | -1.4580                         | -0.7140         | -0.7990         |
| $\Lambda/\Lambda$                             | 0.7361                    | 0.74   | 0.05                                       | -0.0639          | -0.0786                   | -0.0580         | -0.1016                         | -0.0918         | -0.1196         |
| $\bar{p}/p$                                   | 0.6925                    | 0.71   | 0.06                                       | -0.2832          | -0.2909                   | -0.4915         | -0.4751                         | -0.4121         | -0.4200         |
| $K^+/K^-$                                     | 1.0708                    | 1.103  | 0.025                                      | -1.2304          | -1.2864                   | -0.9170         | -1.0373                         | -1.1507         | -1.2051         |
| $K^-/\pi^-$                                   | 0.1956                    | 0.181  | 0.025                                      | 0.5166           | 0.5850                    | -0.1989         | 0.3956                          | 0.7844          | 1.0511          |
| $K^+/\pi^+$                                   | 0.2081                    | 0.201  | 0.025                                      | 0.2231           | 0.2849                    | -0.4912         | 0.1244                          | 0.5095          | 0.7046          |
| model prediction ratios                       |                           |        |  |                  |                           |                 |                                 |                 |                 |
| $\Lambda(1520)/\Lambda$                       |                           | N/A    |  | 0.0390           | 0.0383                    | 0.0567          | 0.0568                          | 0.0510          | 0.0528          |
| $\Delta^{++}/p$                               |                           | N/A    |  | 0.1023           | 0.1030                    | 0.1322          | 0.1260                          | 0.1209          | 0.1195          |
| $\phi/K^-$                                    |                           | N/A    |  | 0.1374           | 0.1353                    | 0.1379          | 0.1346                          | 0.1498          | 0.1414          |
| $K^*(892)/K^-$                                |                           | N/A    |  | 0.2260           | 0.2297                    | 0.3100          | 0.3023                          | 0.2907          | 0.2893          |
| $f_0(980)/\phi$                               |                           | N/A    |  | 0.2020           | 0.2679                    | 0.4083          | 0.4619                          | 0.3005          | 0.3858          |
| $\Sigma^*(1385)/\Xi$                          |                           | N/A    |  | 0.5139           | 0.5498                    | 0.7209          | 0.7258                          | 0.6202          | 0.6605          |
| $\Xi^*(1530)/\Xi$                             |                           | N/A    |  | 0.2579           | 0.1750                    | 0.2857          | 0.2879                          | 0.2804          | 0.2837          |
| $\Theta^+(1540)/\Xi^*$                        |                           | N/A    |  | 1.0875           | 1.6870                    | 0.5896          | 0.5699                          | 0.4964          | 0.5119          |
| statistical parameters                        |                           |        |  |                  |                           |                 |                                 |                 |                 |
|   | $T$ [MeV]                 |        |  | $133 \pm 10$     | $135 \pm 12$              | $158 \pm 13$    | $0.157 \pm 15$                  | $152 \pm 16$    | $153 \pm 23$    |
|   | $10^4(\lambda_q - 1)$     |        |  | $708 \pm 342$    | $703 \pm 337$             | $735 \pm 390$   | $730 \pm 382$                   | $724 \pm 373$   | $721 \pm 363$   |
|   | $\lambda_s^1$             |        |  | 1.03132973       | 1.03203555                | 1.02636207      | 1.02788897                      | 1.0295346       | 1.0300848       |
|   | $\gamma_q$                |        |  | $1.66 \pm 0.013$ | $1.65 \pm 0.030$          | 1               | 1                               | 1               | 1               |
|   | $\gamma_s$                |        |  | $2.41 \pm 0.61$  | $2.28 \pm 0.46$           | 1               | 1                               | $1.17 \pm 0.30$ | $1.10 \pm 0.25$ |
|   | $10^4(\lambda_{I_3} - 1)$ |        |  | $30 \pm 305$     | $28 \pm 293$              | $59 \pm 564$    | $53 \pm 508$                    | $64 \pm 525$    | $59 \pm 481$    |
| fit relevance                                 |                           |        |  |                  |                           |                 |                                 |                 |                 |
|   | $N - p = \text{DoF}$      |        |  | 16-5             | 16-5                      | 16-3            | 16-3                            | 16-4            | 16-4            |
|   | $\chi^2/\text{DoF}$       |        |  | 0.4243           | 0.4554                    | 1.0255          | 0.8832                          | 0.6067          | 0.7301          |
|   | statistical significance  |        |  | 0.9461           | 0.9307                    | 0.4225          | 0.5705                          | 0.8385          | 0.7232          |

## STRANGENESS / NET BARYON NUMBER $s/b$

Baryon number  $b$  is conserved, strangeness could increase slightly in hadronization.  $s/b$  ratio probes the mechanism of primordial fireball baryon deposition and strangeness production. Ratio eliminates dependence on reaction geometry.

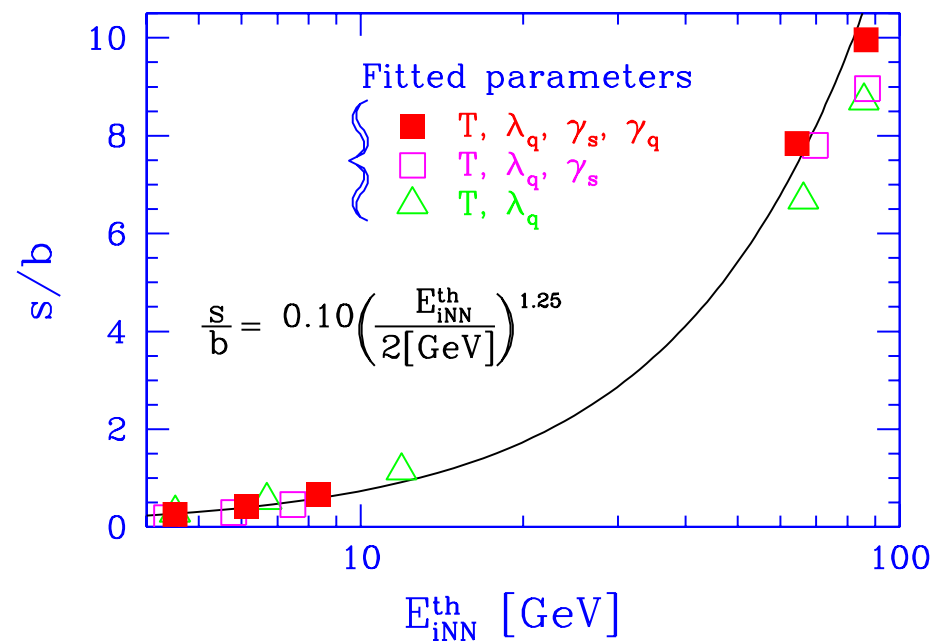
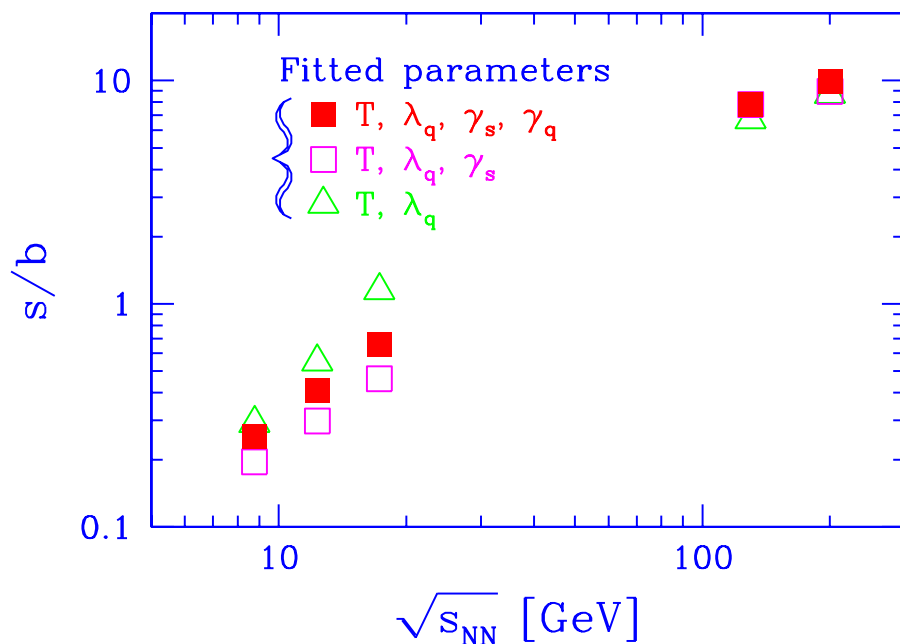
## STRANGENESS / ENTROPY CONTENT $s/S$

Strangeness  $s$  and entropy  $S$  produced predominantly in early hot parton phase. Ratio eliminates dependence on reaction geometry. Strangeness and entropy could increase slightly in hadronization.

## HADRON PHASE SPACE OVERPOPULATION

$\gamma_s, \gamma_q$  allow correct measure of yields of strangeness and baryon number, probe dynamics of hadronization, allow fast breakup without 'mixed phase'

## FROM SPS to RHIC: STRANGENESS vs NET BARYON CONTENT



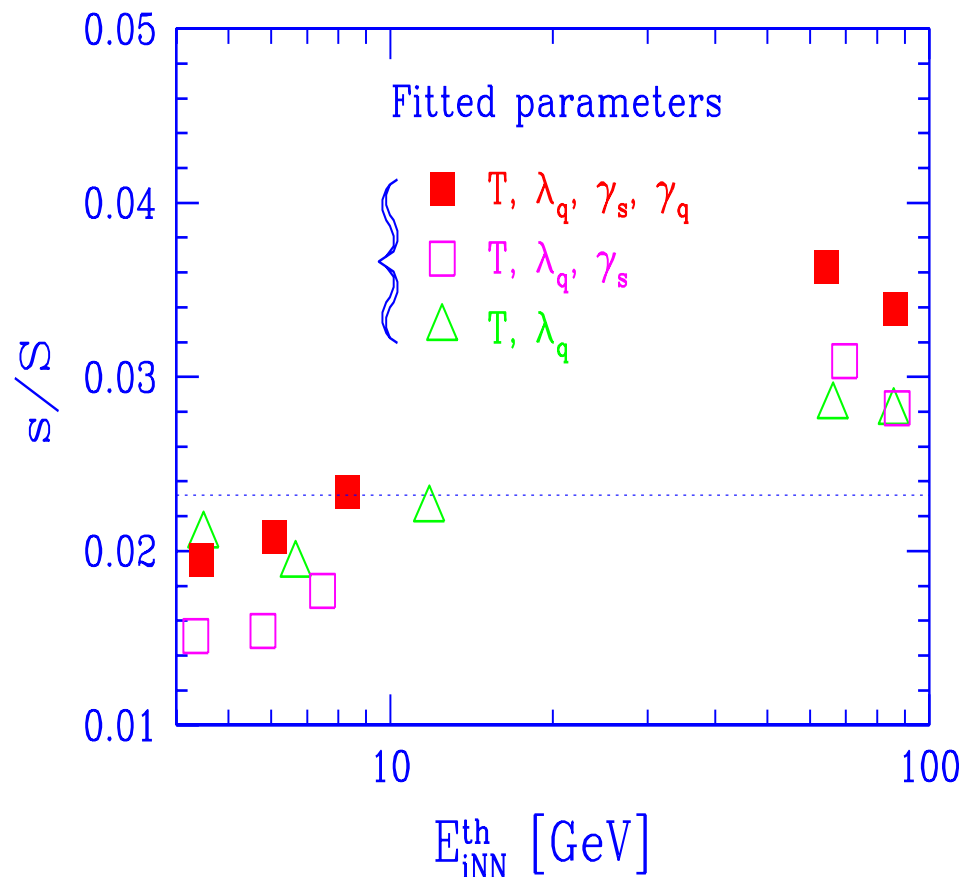
Strangeness per thermal baryon participating in the reaction grows rapidly and continuously. **Gluon based thermal QCD production mechanism UNDERSTOOD.**

Strangeness production maybe rises faster than entropy.  
YIELD MUCH GREATER THAN IN NN-REACTIONS

### OUTLOOK:

Soon at LHC – charm takes over from strangeness – an experimental challenge

**YET MORE INTERESTING: STRANGENESS/ENTROPY CONTENT**

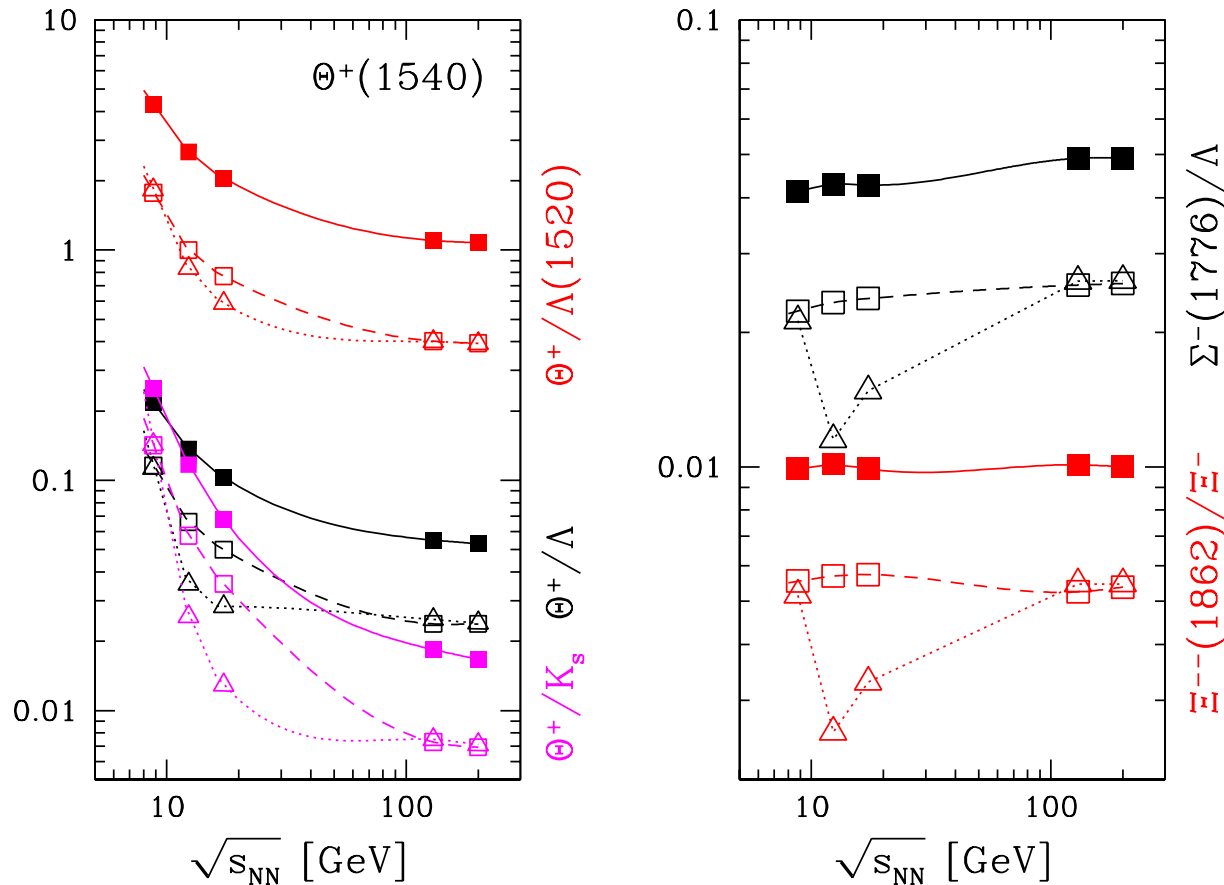


From AGS to SPS: step up by 50% (not shown) and second step-up by 50% in strangeness per entropy between SPS and RHIC  
 Strangeness production rises with energy faster than production of entropy.

New physics at RHIC compared to SPS??  
 New physics at SPS compared to AGS??

# Pentaquarks

Our systematic study of chemical properties at hadronization allows to explore the rate of production of pentaquarks which are very sensitive to chemical potentials:  $\Theta^+(1540)[uudd\bar{s}]$  ('wrong strangeness' baryon) and  $\Xi^{--}(1862)[ssqq\bar{q}]$ ,  $\Sigma^-(1776?)[sqqq\bar{q}]$ . (PRC68, 061901 (2003), hep-ph/0310188)



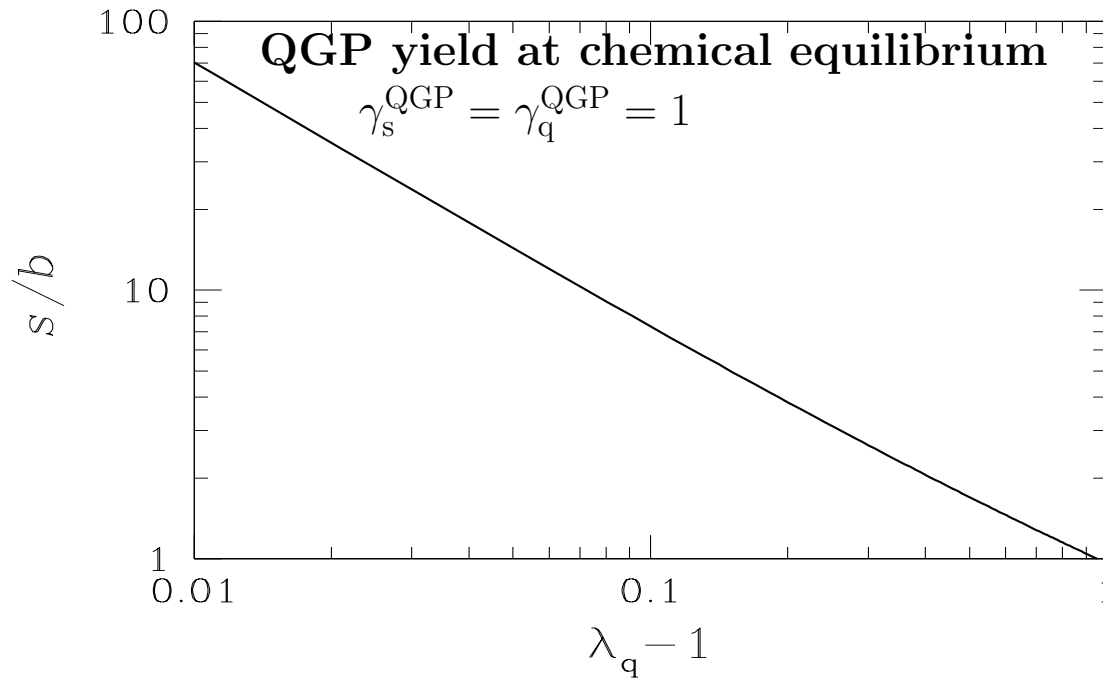
Expected relative yield of  $\Theta^+(1540)$  (left);  $\Xi^{--}(1862)$  and  $\Sigma^-(1776?)$  (right), based on statistical hadronization fits at SPS and RHIC: solid lines  $\gamma_s$  and  $\gamma_q$  fitted; dashed lines  $\gamma_s$  fitted,  $\gamma_q = 1$ ; dotted lines  $\gamma_s = \gamma_q = 1$ .

## NOW COMPARE TO STRANGENESS YIELD IN QGP and $\gamma_s^{\text{QGP}}/\gamma_q^{\text{QGP}}$

$$\frac{\rho_s}{\rho_b} = \frac{s}{q/3} = \frac{\gamma_s^{\text{QGP}} \frac{3}{\pi^2} T^3 (m_s/T)^2 K_2(m_s/T)}{\gamma_q^{\text{QGP}} \frac{2}{3} (\mu_q T^2 + \mu_q^3/\pi^2)}, \rightarrow \frac{s}{b} \simeq \frac{\gamma_s^{\text{QGP}}}{\gamma_q^{\text{QGP}}} \frac{0.7}{\ln \lambda_q + (\ln \lambda_q)^3/\pi^2}.$$

assumption:  $\mathcal{O}(\alpha_s)$  interaction effects cancel out between  $b, s$

We consider  $m_s = 200$  MeV and hadronization  $T = 150$  MeV,



At SPS  $\lambda_q=1.5-1.6$ , implies  $s/b \simeq 1.5$ .

**Observation:**  $s/b \simeq 0.75 \rightarrow \gamma_s^{\text{QGP}}/\gamma_q^{\text{QGP}} = 0.5$  at SPS

Similarly for RHIC at  $\sqrt{s_{\text{NN}}} \geq 130$  GeV we have  $1 \leq \lambda_q \leq 1.1$  and a comparison of the actual  $s/b$  yield allows to estimate  $\gamma_s^{\text{QGP}}/\gamma_q^{\text{QGP}} = 0.7-0.8$  at RHIC-130/200.

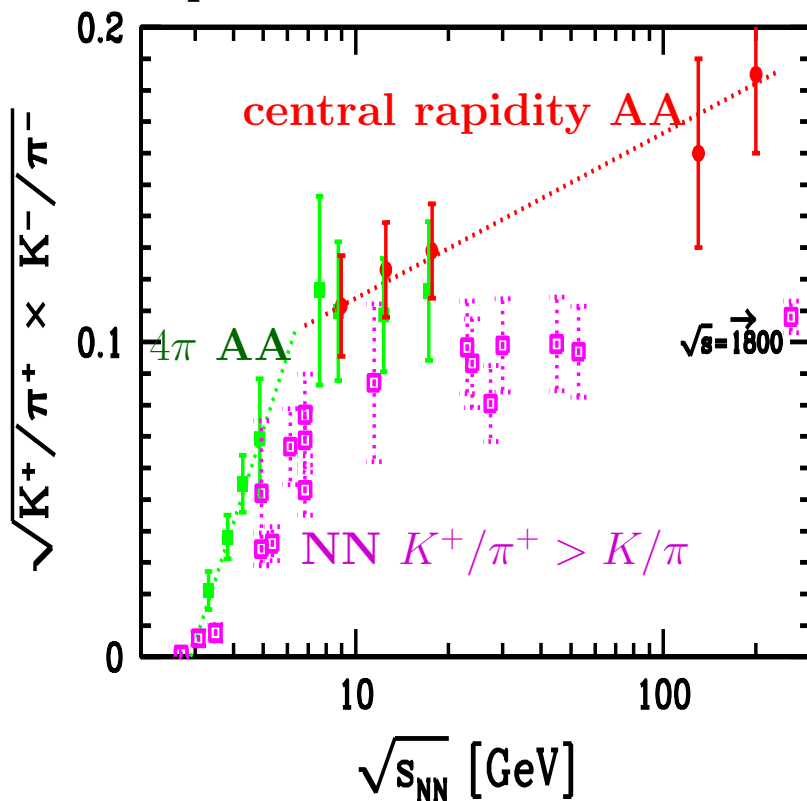
## Probing strangeness excitation by ratio $K/\pi$

The particle yield products

$$K \equiv \sqrt{K^+(u\bar{s})K^-(\bar{u}s)} \propto \sqrt{\lambda_u/\lambda_s \lambda_s/\lambda_u}$$

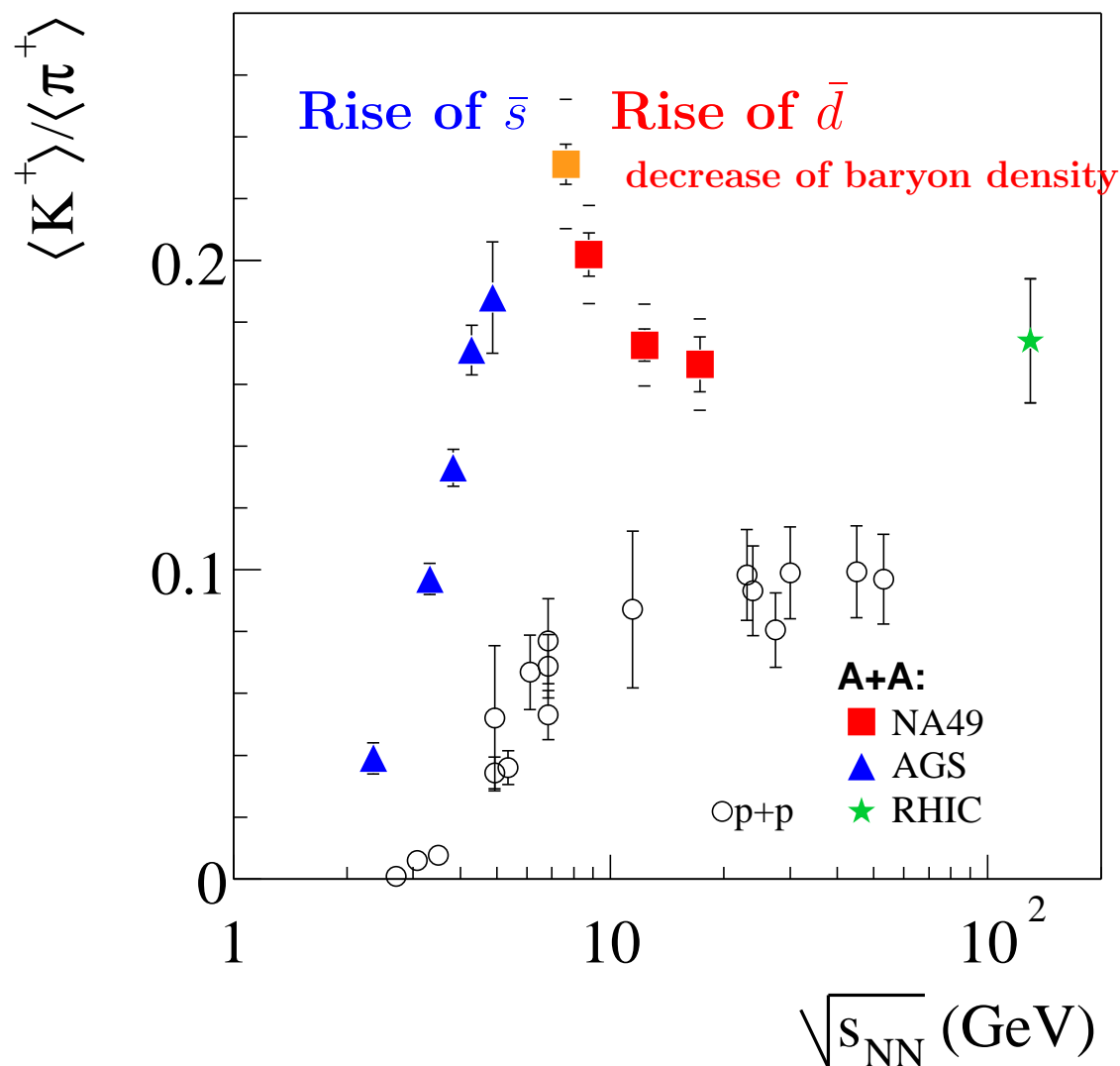
$$\pi \equiv \sqrt{\pi^+(u\bar{d})\pi^-(\bar{u}d)} \propto \sqrt{\lambda_u/\lambda_d \lambda_d/\lambda_u}$$

are less dependent on chemical conditions including baryon density.



There is a notable enhancement in  $K/\pi$  above the  $K^+/\pi^+$  ratio recorded in  $pp$  reactions, which provides an upper limit on  $K/\pi$ . There is a clear change in the speed of rise in the  $K/\pi$  ratio at the lower energy limit at SPS; This combined with change in nuclear compression results in a peak in the  $K^+/\pi^+$ .

# NA49/Marek Gaździcki STUDY $\bar{s}/\bar{d}$ ENHANCEMENT



## Is QGP discovered??

Predicted QGP behavior confirmed by strangeness and strange antibaryon enhancement experiments, verifies strange quark mobility. Enhanced source entropy content consistent with gluon degrees of freedom, expected given strangeness enhancement. Chemical properties consistent with sudden hadron production in fast breakup of QGP.

---

Furthermore: quark coalescence explains features of non-azimuthally symmetric strange particle production. Early thermalization and strange quark participation in matter flow.

---

Strangeness excitation function fingerprints QGP as the new state of matter:  
Probable onset of 'valon' quark deconfinement at AGS;

---

## FINAL REMARKS

The deconfinement specific hadronic 'deep' probes are entropy and strangeness. These probes are fully consistent with deconfinement/QGP at SPS and at RHIC

---

We have good control of statistical models and chemical potentials, particle abundances, but not yet of phase transformation dynamics.